Refinement of magnetic domains in $FeTbGe_2O_7$

I. Rosales[a], C. Thions-Renero[a], E. Orozco[a], M. T. Fernández-Díaz[b] and L. Bucio[a]
[a]*Instituto de Física, Universidad Nacional Autónoma de México,*
Apartado Postal 20-364, 01000, México, DF, México,
Tel. :(52+55) 56225000; fax: (52+55) 56225000.
e-mail: bucio@fisica.unam.mx
[b]*Institut Laue-Langevin, BP 156X, Grenoble Cedex, France.*

Received 30 July 2015; accepted 14 August 2015

Antiferromagnetic polycrystalline $FeTbGe_2O_7$ compound presents an ordered magnetic phase when its temperature decreases below the Néel temperature T_N = 42 K. By mean of Rietveld refinement of collected neutron diffraction data, the broadened part of the magnetic peaks was modeled in order to analyze the effect of average size of magnetic domains on the evolution of magnetic structure with temperature. The rise of the magnetic structure was found to be sensitive to the shortening of distances along the b-axis between the magnetic atoms located in the bc-sheets of the layered structure. When the magnetic structure is generated, chains along the b-axis of Tb^{3+}-Tb^{3+} atoms are antiferromagnetically coupled. At the same time, ferromagnetic coupling along the c-axis between Tb^{3+}-Fe^{3+} atoms located in contiguous chains, couples all the chains along a sheet in the layered structure. The three-dimensional magnetic structure is reached by the ferromagnetic coupling between the set of sheets parallel to bc in the layered structure. A correlation between the size of the magnetic domain and the reach of the saturation value for the magnetic moment for Fe^{3+} is suggested. The magnetic reflections appear below 42 K and were modelled independently from those reflections coming from the crystal structure ignoring the effect of magnetostriction.

Keywords: Thortveitite; nanophase; antiferromagnetic; neutron diffraction.

El compuesto policristalino $FeTbGe_2O_7$ antiferromagnético presenta una estructura magnética cuando su temperatura desciende por debajo de la temperatura de Néel T_N = 42 K. Por medio del refinamiento Rietveld de los datos de difracción de neutrones, se modeló el ensanchamiento de las reflexiones magnéticas con el fin de analizar el efecto del tamaño medio de los dominios magnéticos y la evolución de la estructura magnética con la temperatura. Se encontró que el desarrollo de la estructura magnética es sensible al acortamiento de distancias a lo largo del eje b de átomos magnéticos situados sobre planos paralelos a bc en la estructura laminar. Cuando se genera la estructura magnética, se forman cadenas de átomos Tb^{3+}-Tb^{3+} a lo largo del eje b que se acoplan antiferromagneticamente. A su vez, se establece un acoplamiento ferromagnético a lo largo del eje c entre átomos Tb^{3+}-Fe^{3+} que se sitúan en cadenas contiguas en todas las cadenas que forman una hoja en la estructura laminar. La estructura magnética tridimensional se logra por el acoplamiento ferromagnético entre el conjunto de hojas paralelas a bc en la estructura en capas. Se sugiere una correlación entre el tamaño del dominio magnético y el alcance del valor de saturación para el momento magnético de Fe^{3+}. Las reflexiones magnéticas que aparecen por debajo de 42 K pudieron modelarse independientemente de las reflexiones procedentes de la estructura cristalina, ignorando el efecto de la magnetostricción.

Descriptores: Thortveitita; nanofase; antiferromagnetismo; diffracción de neutrones.

PACS: 61.05.F-; 61.46.-w; 75.47.Lx; 75.50.Ea

1. Introduction

Although originally conceived for dealing with nuclear and magnetic structures, in which a set of parameters are refined following a least squares procedure [1], the Rietveld method has also been successfully applied for microstructural analysis, which typically includes crystallite size and micro strain effects [2,3]. This analysis takes advantage on the way that the microstructural effects contribute to the broadened peak shapes obtained from the X-ray or neutron powder diffraction data [4,5]. For conventional refinements, the well-known pseudo-Voigt function (a linear combination between a gaussian and a lorentzian function) is the most typical mathematical function that gives the best fit to the shapes of the Bragg peaks obtained from X-ray or neutron powder diffraction experiments. In such cases, each peak has a full width at half-maximum (FWHM) given by the Caglioti, Paoletti and Ricci formula [6]

$$\mathrm{FWHM}^2 = u\tan^2\theta + v\tan\theta + w \qquad (1)$$

where u, v and w are the refinable parameters which have no physical meaning under the scope of a microstructural model (*i.e.* crystallite size, lattice distortions, etc.). At first instance, the solely refinement of the profile parameters u, v and w is enough to successfully reach a detailed structural information (crystallographic or magnetic). Thompson, Cox and Hastings [2] reported a modified pseudo Voigt function in which the maximum physically significant information on the sample microstructure, is performed by a correct convolution of instrumental function with intrinsic profile function (both considered Voigtians). In the FULLPROF program for Rietveld refinements [7], the modified pseudo Voigt function has gaussian (FWHM_G) and lorentzian (FWHM_L) components of FWHM which have the expressions

$$\mathrm{FWHM}_G^2 = [u + (1-\zeta)^2 D_{ST}^2] \tan^2\theta + v\tan\theta + w + \frac{I_G}{\cos^2\theta}$$

$$\mathrm{FWHM}_L = [\chi + \zeta D_{ST}] \tan\theta + \frac{y+F}{\cos\theta}$$

When an instrumental resolution function is given [7] the v and w parameters are fixed to zero and the remaining parameters in the previous formula, u, x have a meaning in terms of strain; or y, I_G in terms of size. D_{ST} and F are functions defined according to specific models for anisotropic strain and size contributions respectively which include additional refinable parameters. The y parameter provides a size value $\langle S\rangle$ given by 180 $k\lambda/(\pi y)$; where k is the FWHM - integral breath ratio, which is $2/\pi$ for a lorentzian. With such value for k, $\langle S\rangle$ represents the volume averaged crystallite diameter in all directions.

For the case of magnetic reflections, if the broadening of the diffraction peaks is considered entirely due to the interaction of the neutron spin with the magnetic moments of the atoms constituting a magnetic structure, then the mean size of magnetic domains in the sample can be estimated, which allows to obtain relevant information concerning the magnetic microstructure of the sample under study.

A case of magnetic structure has been reported for the layered compound $FeTbGe_2O_7$ [8] as well as its crystal structure, which is described as belonging to the monoclinic system with space group $P2_1/m$ (No. 11). This structure is related with that of mineral thortveitite, $Sc_xY_{1-x}Si_2O_7$, whose symmetry is described by the space group $C2/m$ (No. 12). Its arrangement can be explained as follows: Sc^{3+} and Y^{3+} cations are at the centre of an octahedron and share statistically the same and unique crystallographic position for these atoms. This kind of octahedra is disposed forming a honeycomb-like arrangement along the ab planes. In turn, these ScO_6/YO_6 octahedral layers are held together by sheets of isolated diorthogroups Si_2O_7 constituted by two tetrahedra sharing a common vertex (the bridging oxygen, in which the Si-O-Si angle is 180°). In the crystal structure of $FeTbGe_2O_7$, the bridging oxygen is distorted in such a way that lies enough closer of a Tb^{3+} cation, becoming part of its coordination sphere. Thereby the Tb^{3+} cation changes its coordination with oxygen from 6 to 7. Consequently, the Ge-O-Ge angle is not 180°, and the unique crystallographic position for Tb^{3+}/Fe^{3+} cations splits into two independent crystallographic positions: one for Tb^{3+} (seven-coordinated) and the other for Fe^{3+} (six-coordinated); the symmetry is now described by the space group $P2_1/m$ [8]. The magnetic structure reported for $FeTbGe_2O_7$ shows a simultaneous three dimensional antiferromagnetic ordering on Fe and Tb sublattices at 42 K, the Néel temperature [8]. The reported magnetic structure lacks detailed information concerning the behaviour of the magnetic moment components of the involved atoms as the cell parameters changes into the temperature range studied. The aim of this work is to carry out a careful description in terms of the evolution of the magnetic microstructure, -the mean size of magnetic domains in the sample-, the cell parameters (the crystal structure distortion) and magnetic moment components along the crystallographic base vectors as temperature changes from 1.7 and 200 K by Rietveld refinement of the neutron diffraction data.

2. Experimental

$FeTbGe_2O_7$ was prepared as described in Ref. 8 and its neutron powder diffraction patterns (NPD) were collected on the high flux and medium resolution D1B powder diffractometer at Institut Laue - Langevin, Grenoble. On about 10 g of sample was introduced in a cylindrical vanadium can which was held in a liquid helium cryostat for measurements at low temperatures from 1.7 to 200 K using a neutron beam with 2.52 Å wavelength. The neutron powder diffraction patterns (NDP) were approximately collected each 1 K in 5 min within angular range $15 \leq 2\theta \leq 85°$ on intensity counts collected in a ^{3}He multidetector.

Rietveld method implemented in FULLPROF program [7] was used to refine the magnetic structure on each NPD pattern using the pseudo Voigt function modified by Thompson, Cox and Hastings. The refinement began with the 1.7 K NPD pattern in such a way that the results obtained in this first refinement were used as starting parameters to refine the next NPD. The successive refinements were carried out with this procedure taking into account the presence of two phases: one due to the crystal structure contribution, and the other due to the magnetic contribution. These refinements finished at 42 K NPD when there are very weak magnetic peaks not suitable for a refinement. This first set of refinements were used to perform the analysis of the mean size of magnetic domains in the sample, the cell parameters (the crystal structure distortion) as well as the magnetic moment components along the crystallographic base vectors at temperatures below 42 K.

In the next successive refinements until 200 K only the crystal structure contribution to the observed Bragg peaks was considered. These set of refinements were used to obtain the variation of the cell parameters from above 42 K until 200 K.

The background was fitted using a refinable quadratic polynomial function in 2θ. The magnetic form factors for Tb and Fe were taken from those reported by Brown [9].

3. Results and Discussion

Figure 1 displays the variation of lattice parameters with temperature from 1.7 to 200 K. The first graph (Fig. 1a), shows an almost constant comportment for lattice parameter a on

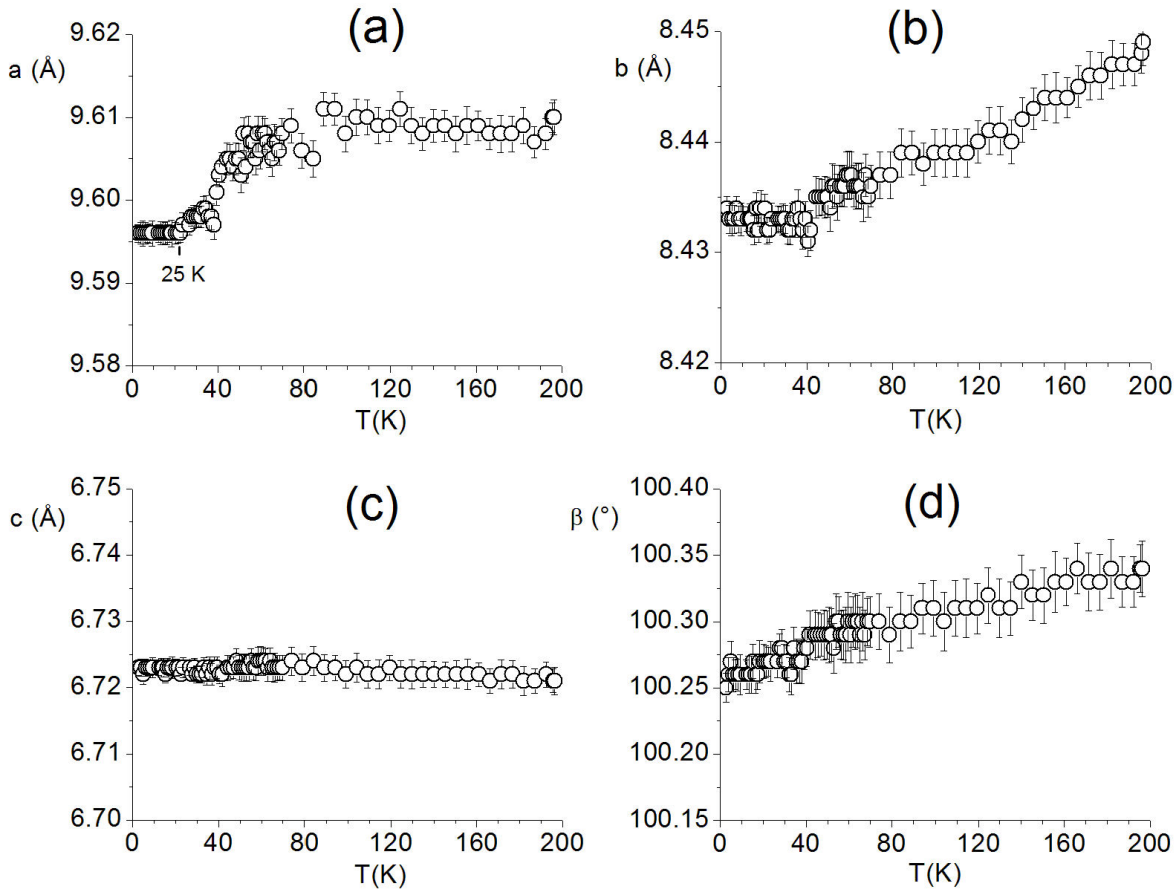

FIGURE 1. Thermal variation on a, b, c and β lattice parameters.

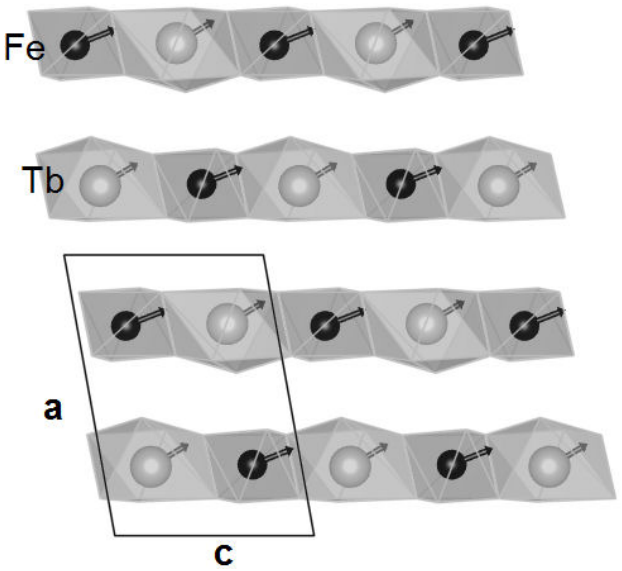

FIGURE 2. Ferromagnetic coupling between parallel bc planes along the a-axis.

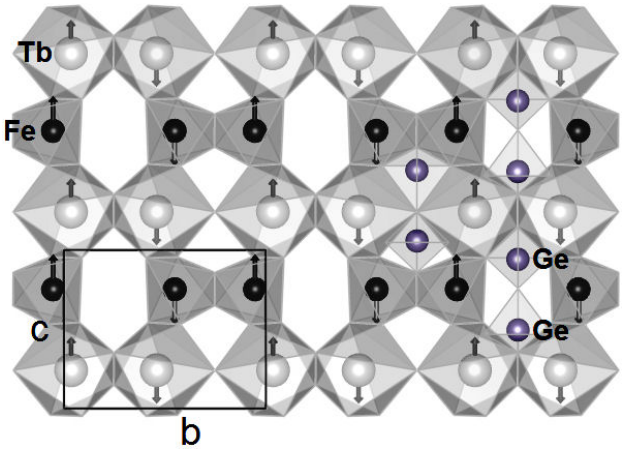

FIGURE 3. Magnetic moments of Fe^{3+} and Tb^{3+} lying ferromagnetically coupled along c axis on bc planes while antiferromagnetic couplings between Fe^{3+}-Fe^{3+} and Tb^{3+}-Tb^{3+} along b axis are lying also on bc planes at 1.7 K temperature.

the range below 25 K and after 42 K, varying suddenly around the Néel temperature. On their turn, b and β parameters (Figs. 1b and 1d) show approximately a linear behaviour; while c parameter practically keeps constant all the temperature range (Fig. 1c). These very important structural changes are not clearly observed in Ref. 8, since the information reported in the paper, only covers a temperature range from 2 to 60 K: the graphs reported in the reference show a practically constant variation with temperature for all the parameters; the only exception is the a parameter, which changes its constant

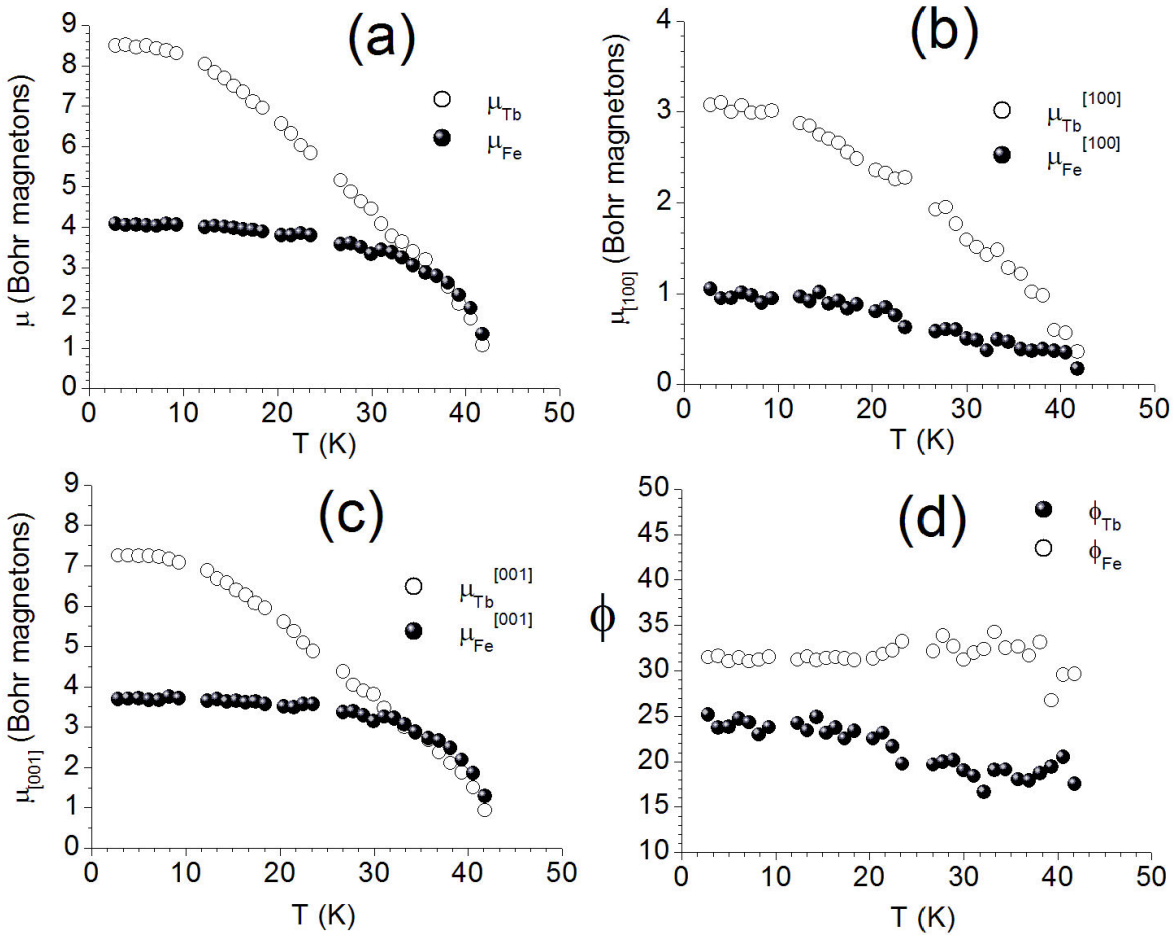

FIGURE 4. Thermal evolution of the ordered magnetic moments of Fe^{3+} and Tb^{3+} in $FeTbGe_2O_7$: (a) magnetic moment moduli; (b) magnetic moment component along [100] direction; (c) magnetic moment component along [001] direction; (d) Φ is the angle between the magnetic moment and the [001] direction.

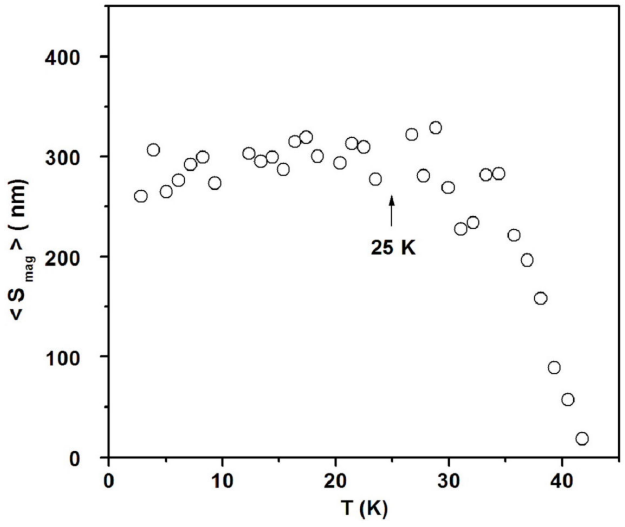

FIGURE 5. Volume averaged on magnetic domain crystallite diameter mag $\langle S_{\rm mag}\rangle$ as function of temperature.

its constant behaviour to increase approximately after 30 K. In general, these observations suggest that as the magnetic structure is destroyed, the sheets forming the layered structure, suddenly moves away one to another along the a-axis with a shear displacement along [001] direction giving rise to an abrupt change of the a-parameter around the Néel temperature (Fig. 2). The shear effect agrees with the linear increase of the monoclinic angle β.

The magnetic structure of $FeTbGe_2O_7$ compound shows a simultaneous three-dimensional antiferromagnetic ordering on Fe and Tb sublattices at 42 K, the Néel temperature [8] (Figs. 2 and 3). At 1.7 K the magnetic moments reported in Ref. 8 for Fe^{3+} and Tb^{3+} are 3.91(7) and 7.98(8) $\mu_{\rm B}$ (Bohr magnetons) respectively, and lies ferromagnetically coupled along c axis on bc planes (Fig. 3). In the refinements reported here (taking into account the microstructural effects of the magnetic domains), we have obtained 4.08(7) and 8.50(8) $\mu_{\rm B}$ (Bohr magnetons) for the magnetic moments of Fe^{3+} and Tb^{3+} respectively at 2.8 K temperature. Couplings between Fe^{3+}-Fe^{3+} and Tb^{3+}-Tb^{3+} are antiferromagnetic along b axis on bc planes; and occurs in pairs in case of Fe-Fe interactions (Fig. 3). On the other hand, coupling between parallel bc planes was found to be ferromagnetic along the a-axis with relatively small components in a direction (Fig. 2).

The variations of the magnetic moments for Fe^{3+} and Tb^{3+} cations with temperature along the main crystallographic directions have been examined in order to relate them with the corresponding changes measured for the unit cell parameters with temperature. Variations of the magnetic moment moduli with temperature for Fe^{3+} and Tb^{3+} are presented in Fig. 4a. Below 25 K the magnetic moment moduli for Fe^{3+} atoms show a saturation effect, whereas for Tb^{3+} the saturation is observed below 8 K. The corresponding components of the magnetic moments along [100] and [001] directions are displayed in Figs. 4b and 4c respectively; the angle between the magnetic moment and the c-axis (φ) as function of temperature appears in Fig. 4d. Both magnetic moments for Fe^{3+} and Tb^{3+} have a major components along the c-axis, whose values becomes larger as temperature increases and reaches a saturation limit close to the Néel temperature. Since φ angle tends linearly to zero with temperature for Fe^{3+} and is approximately constant for Tb^{3+}, there is a remarkable strong tendency for alignment of the magnetic moment for Fe^{3+} towards c-axis in comparison with that for Tb^{3+}.

When the arrangement of magnetic moments is presented below 42 K, the distance along b-axis involved in the antiferromagnetic couplings is almost constant. Below 42 K, we could not observed significative changes in the interatomic distances for Fe^{3+}-Fe^{3+}, Tb^{3+}-Fe^{3+}, or Tb^{3+}-Tb^{3+}, obtained from the diffractograms measured at temperatures in the range lower than 42 K. These results agree with the approximately constancy behaviour of b and c parameters below 42 K. This last fact allow us to ignore the effect of broadening by magnetostriction of the magnetic Bragg peaks measured in the neutron difractograms below 42 K. Then we could consider that the broadening of the diffraction peaks was entirely due to the interaction of neutron spins with the magnetic ordering in the several planes of the material. Above 42 K, when there is no magnetic structure, a linear variation of b-parameter was shown by the sample, while c-parameter was kept constant from 1.7 to 200 K (Fig. 1c). The interatomic distances involved to give the magnetic interactions appear along planes parallel to the bc plane; *i.e.* the relevant changes in the atomic coordinates related with the magnetic interactions for the magnetic atoms are y and z.

The refinement of isotropic particle size broadening y, in case of magnetic peaks, allows us to determinate the "volume averaged on magnetic domain crystallite diameter" $\langle S_{\text{mag}} \rangle$. The last could be interpreted as the maximum effective distance at which magnetic ordering is reached forming a domain. The plot of $\langle S_{\text{mag}} \rangle$ versus temperature is show in Fig. 5. It can be seen that below 25 K, $\langle S_{\text{mag}} \rangle$ is almost constant and close to 300 nm, while the magnetic moment moduli of Fe^{3+} cations are also constant and near to its saturation value of 4 μ_{B} in this temperature range.

4. Conclusions

As coordinate y exhibit more significative changes than z for the magnetic atoms in the sheet when the sample reaches the Néel temperature as temperature is decreased, the rise of the magnetic structure could be considered basically sensitive to the shortening of distances along the b-axis between the magnetic atoms located in the bc-sheets of the layered structure. Along the b-axis, chains of antiferromagnetically coupled Tb^{3+}-Tb^{3+} atoms are formed and linked one to another by ferromagnetically coupled Tb^{3+}-Fe^{3+}-Tb^{3+} atoms along the c-axis. It can be suggested a correlation between the size of the magnetic domain and the reach of the saturation value for the magnetic moment for Fe^{3+}. Below 42 K, magnetic reflections appear and were modelled independently from those reflections coming from the crystal structure by the modified pseudo Voigt function and ignoring the effect of magnetostriction. By this way, we are able to estimate the behaviour of the mean size of magnetic domains in the sample in the cited temperature range and improve the results obtained for the magnetic structure and its change with temperature.

Acknowledgments

Authors acknowledge the financial support of the Consejo Nacional de Ciencia y Tecnologia (CONACYT) project CB-2011/167624 and DGAPA-PAPIIT IN-101414.

1. H.M. Rietveld, *J. Appl. Cryst.* **2** (1969) 65.
2. P. Thompson, D.E. Cox and J.B. Hastings *J. Appl. Cryst.* **20** (1987) 79.
3. Th. De Keijser, E.J. Mittemeijer and H.C.F. Rozendaal *J. Appl. Cryst.* **16** (1983) 309.
4. B.E. Warren *X-ray diffraction*. Addison-Wesley, Massachusetts, (1969).
5. A. Guinier, *Théorie et technique de la Radiocristallographie*. Dunod, Paris, (1964).
6. G. Caglioti, A. Paoletti and F.P. Ricci *Nucl. Instrum.* **3** (1958) 223.
7. J. Rodríguez Carvajal 1990 "*FULLPROF: A Program for Rietveld Refinement and Pattern Matching Analysis*", Abstracts of the Satellite Meeting on Powder Diffraction of the XV Congress of the International Union of Crystallography, Toulouse, France, (1990) p. 127.
8. C. Cascales, L. Bucio, E. Gutiérrez-Puebla, I. Rasines, and M.T. Fernández-Díaz, *Phys. Rev. B.* **57** (1998) 5240.
9. P.J. Brown, Institut Laue Langevin Report SP88BR5016, (1988).